Ferromagnetism in Twinned Pt Nanoparticles Obtained by Laser Ablation

M. A. García,[†,‡] M. L. Ruiz-González,[§] G. F. de la Fuente,[||] P. Crespo,[†,‡] J. M. González,[†,⊥] J. Llopis,[‡] J. M. González-Calbet,*[,†,§] M. Vallet-Regí,[†,#] and A. Hernando[†,‡]

Instituto de Magnetismo Aplicado, ADIF-UCM-CSIC, P.O. Box 155, 28230 Las Rozas, Madrid, Spain, Depto. Física de Materiales, UCM, 28040 Madrid, Spain, Depto. de Química Inorgánica I, UCM, 28040 Madrid, Spain, Laboratorio de Procesado de Materiales por Láser, Instituto de Ciencia de Materiales de Aragón, Universidad de Zaragoza-CSIC, María de Luna 3, 50018 Zaragoza, ICMM-CSIC, c/Sor Juana Inés de la Cruz s/n, 28049 Madrid, Spain, and Depto. de Química Inorgánica y Bioinorgánica, UCM, 28040 Madrid, Spain

Received July 25, 2006. Revised Manuscript Received December 13, 2006

In this paper, we report on the preparation and magnetic properties of small Pt nanoparticles (2−5 nm size). The control of the preparation conditions allow the physical properties of the nanoparticles to be tuned, giving rise to properties different from those of bulk Pt. We show here the first experimental observation of ferromagnetic behavior for carbon-coated platinum nanoparticles with coercivity up to room temperature (i.e., surprisingly there are no superparamagnetic effects despite the small size of the nanoparticles). Measurements of the surface plasmon resonance showed the presence of itinerant electrons. TEM studies confirmed that the nanoparticles exhibit a large concentration of twin boundaries which reduce the surface energy. The lack of cubic symmetry at the twin boundaries could give rise to permanent magnetic moments. The large spin−orbit coupling of platinum accounts for a huge magnetic anisotropy and therefore for the surprisingly high blocking temperature, above 300 K. The relationship of the magnetic properties with the particle structure is also discussed.

Introduction

Nanoparticles (NPs) are intensively studied nowadays, because these systems present properties different from those of bulk materials. These differences arise mainly from the large fraction of atoms located at the NP surface, which is not negligible (as is the case for bulk materials), and from the so-called size effects: when the typical lengths of some phenomena are within the same order of magnitude as the particle size, the response of the system strongly depends on this size (that is, on the boundary conditions). As both the size and structure of the nanoparticles are determined by the preparation conditions, the control of the preparation parameters allows the properties of the nanoparticles to be tuned. Many nanoparticle preparative methods, which rely on chemical vapor deposition techniques,[1] chemical precursor decomposition via combustion at high temperatures,[2] self-assembly methods,[3] and other methods,[4] have been widely reported in the literature. They all have interesting advantages, but either lack the desired particle size distribution selectivity or are sufficiently complex to become expensive and excessively time consuming. The laser ablation method presented here, similar to that originally reported by Muñoz et al.,[5] provides several important advantages. These include inexpensive and easy to use equipment, as well as high process efficiency, as a batch of the starting Pt compound is transformed into an NP product within a fraction of a minute. In addition, as typically observed in laser ablation methods, the product obtained is characterized by a narrow size distribution, indicative of a very high selectivity of the laser-induced decomposition process performed here. This is perhaps the most important advantage of this method, since it opens the possibility to obtain, in combination with the proper choice of starting compound, NPs by design.

Recently, it has been shown that NPs of nonferromagnetic bulk materials, such as Pd or Au, exhibit ferromagnetic-like behavior.[6,7] The case of Pd,[6] which is paramagnetic in bulk, can be understood as due to the structural changes when the size of the particle is in the nanometer range. Pd is close to satisfying the Stoner criterion for ferromagnetism, and the

* To whom correspondence should be addressed. E-mail: jgcalbet@quim.ucm.es. Fax: +34 913944352.
† RENFE-UCM-CSIC.
‡ Departamento de Física de Materiales, UCM.
§ Departamento de Química Inorgánica I, UCM.
|| Universidad de Zaragoza-CSIC.
⊥ ICMM-CSIC.
Departamento de Química Inorgánica y Bioinorgánica, UCM.

(1) He, C. N.; Du, X. W.; Ding, J.; Shi, C. S.; Li, J. J; Zhao, N. Q.; Cui, L. *Carbon Rev. Lett.* **2006**, *44*, 2330.
(2) Lin, C. S.; Khan, M. R; Lin, S. D. *J. Colloid Interface Sci.* **2006**, *299*, 678. Saita, S.; Maenosono, S. *Chem. Mater.* **2005**, *17*, 6624.
(3) Lin, X.-M.; Samia, A. C. S. *J. Magn. Magn. Mater.* **2006**, *305*, 100.
(4) Roychowdhury, C.; Matsumoto, F.; Zeldovich, V. B.; Warren, S. C.; Mutolo, P. F.; Ballesteros, M.; Wiesner, U.; Abruña, H. D.; DiSalvo, F. J. *Chem. Mater.* **2006**, *18*, 3365.
(5) Muñoz, E.; de Val, M.; Ruiz-González, M. L.; López-Gascon, C.; Sanjuán, M. L.; Martínez, M. T.; González-Calbet, J. M.; de la Fuente, G. F.; Laguna, M. *Chem. Phys. Lett.* **2006,** *420*, 86. For similar methodology see: Maskrot, H.; Leconte, Y.; Herlin-Boime, N.; Reynaud, C.; Guelou, E.; Pinard, L.; Valange, S.; Barrault, J.; Gervais, M. *Catal. Today* **2006**, *116*, 6.
(6) Sampedro, B.; Crespo, P.; Hernando, A.; Litrán, R.; Sánchez-López, J. C.; López-Cartes, C.; Fernández, A.; Ramirez, J.; González-Calbet, J.; Vallet-Regí, M. *Phys. Rev. Lett.* **2003**, *91*, 237203.
(7) Crespo, P.; Litrán, R.; Rojas, T. C.; Multigner, M.; de la Fuente, J. M.; Sánchez-López, J. C.; García, M. A.; Hernando, A.; Penadés, S.; Fernández, A. *Phys. Rev. Lett.* **2004**, *93*, 087204.

10.1021/cm061740v CCC: $37.00 © 2007 American Chemical Society
Published on Web 01/26/2007

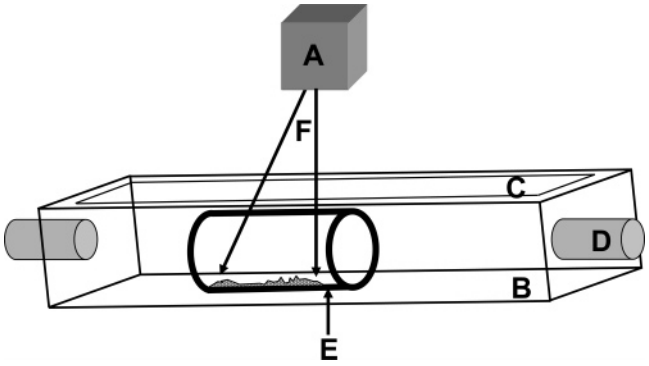

Figure 1. Schematic illustration of the experimental apparatus used for Pt NP laser ablation synthesis. The galvanometer mirror box (A) distributes the laser radiation (F) through a flat field focal lens and a silica window (C) onto the starting Pt compound, placed inside a glass vial (E) and into the portable vacuum chamber (B), fitted with vacuum and entrance ports (D).

small changes in the electronic structure, associated with confinement effects and the presence of twin boundaries, give rise to ferromagnetic behavior. The case of Au[7] is more surprising, as it is a diamagnetic metal with a very low density of states at the Fermi level. In this case, the permanent magnetism appears by selective capping of the NP with strongly interacting thiol groups, giving rise to localization of holes/electrons in the surface of the particle, and by the large spin−orbit interaction of Au atoms. Those results pointed out that the appearance of ferromagnetic behavior in NPs can be due to different mechanisms related to both surface and volume effects.

Although carbon-coated noble metal NPs have been widely used in biology for many applications since they are biocompatible materials,[8] the appearance of ferromagnetism in those NPs is very amazing and could open the possibility to control their movement inside biological tissue or perform very localized heating, increasing their potential applications.

Platinum is a paramagnetic metal, but almost in the limit of ferromagnetic behavior, and thus, the structural changes due to size effects (controlled through the preparation conditions) could modify its magnetic behavior. In this work we show for the first time ferromagnetic behavior at room temperature of small Pt NPs capped with carbon.

Experimental Section

Carbon-coated Pt NPs were obtained by laser ablation. Commercially available *cis*-bis(benzonitrile)dichloroplatinum(II) in 98% purity (Aldrich Chemical Co.) in powder form was used as the ablation target. Figure 1 illustrates the experimental apparatus used in this work. The powder was placed inside an opened glass vial (E) which, in turn, was introduced into a portable vacuum chamber (B) with a thick vitreous silica (Herasil, Schott) rectangular window (C). A Baasel Lasertech Nd:YAG, Q-switched laser emitting at a wavelength of 1064 nm in continuous wave mode, fitted with a galvanometer mirror box (A) with computer-controlled galvanometer mirrors for $x-y$ movement, was used to trigger pyrolysis of the starting material. The production parameters were as follows: 200 mm/s displacement speed, 30 W laser power, 90 μm line fill width combined with 50 μm lines to completely scan a rectangular area over the starting compound, and a wobul (line width oscillation) frequency of 500 Hz. A laser beam waist of 50 μm at the focal spot yields irradiance values of 1.53×10^6 W cm^{-2}, assuming that all the laser radiation is absorbed by the compound target. This laser irradiance level is sufficient to induce plasma formation above the target, according to the range of values reported in the literature.[9] After the laser ablation experiment, no original powder was detected, and the starting product had been converted into a black, fibrous product deposited mainly onto the top wall of the support vial.

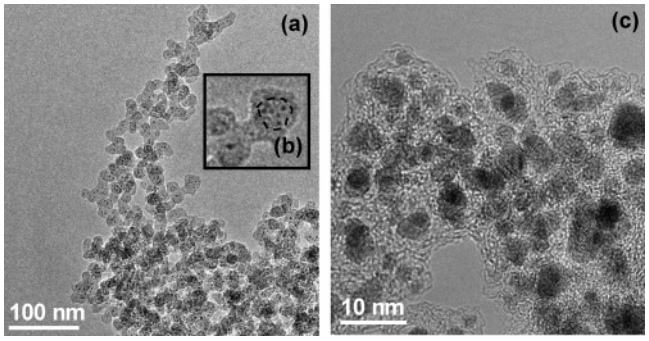

Figure 2. (a) Low-magnification image of the Pt compound, after laser ablation. (b) Enhanced detail of image a, showing the presence of black spots over a gray matrix. (c) HREM image showing Pt nanoparticles embedded on a carbonaceous matrix.

Magnetic characterization has been carried out with a SQUID magnetometer below 350 K. The diamagnetic contribution of the sample holder has been subtracted for obtaining the NP magnetization. The surface plasmon has been measured by means of a UV−vis optical absorption spectrometer.

High-resolution electron microscopy (HREM) was carried out on a JEOL JEM-3000F microscope equipped with an ISIS 300 X-ray microanalysis system (Oxford Instruments) with a LINK "Pentafet" detector for energy dispersive X-ray spectroscopy (EDS) analyses. As EDS gives local information on individual nanoparticles, an average chemical analysis was also performed by atomic absorption. No traces of iron impurities were found, indicating that the iron content must be below 0.01 atom %.

Results and Discussion

A transmission electron microscopy study has been performed to investigate both the morphology and the microstructure of the sample. A low-magnification image, displayed in Figure 2a, shows the presence of gray round particles, of about 20 nm, forming "rosary"- like assemblies, which resemble those observed in the so-called carbon nanofoams.[10] Such reported nanostructures are, indeed, produced after laser ablation of glassy carbon in an Ar atmosphere. Moreover, darker spots, pointed out in Figure 2b, appear over these round particles, requiring HREM characterization to determine the nature of this composite. In this sense, the presence of crystalline particles, black dots, embedded on a carbonaceous matrix—gray round particles—are clearly seen in Figure 2c. The inspection of different areas allows establishment of an average crystalline particle size between 2 and 5 nm. EDS analysis indicates that the crystalline material consists of Pt nanoparticles whose

(8) Fritzsche, W.; Taton, A. T. *Nanotechnology* **2003**, *14*, R63.

(9) Rubahn, H.-G. *Laser Applications in Surface Science and Technology*; Wiley: Hoboken, NJ, 1999. Bauerle, D. *Laser Processing and Chemistry*, 3rd ed.; Springer-Verlag: New York, 2000.

(10) Rode, A. V.; Hyde, S. T; Gamaly, E. G.; Elliman, R. G.; McKenzie, D. R.; Bulcock, S. *Appl. Phys. A* **1999**, *69*, S755.

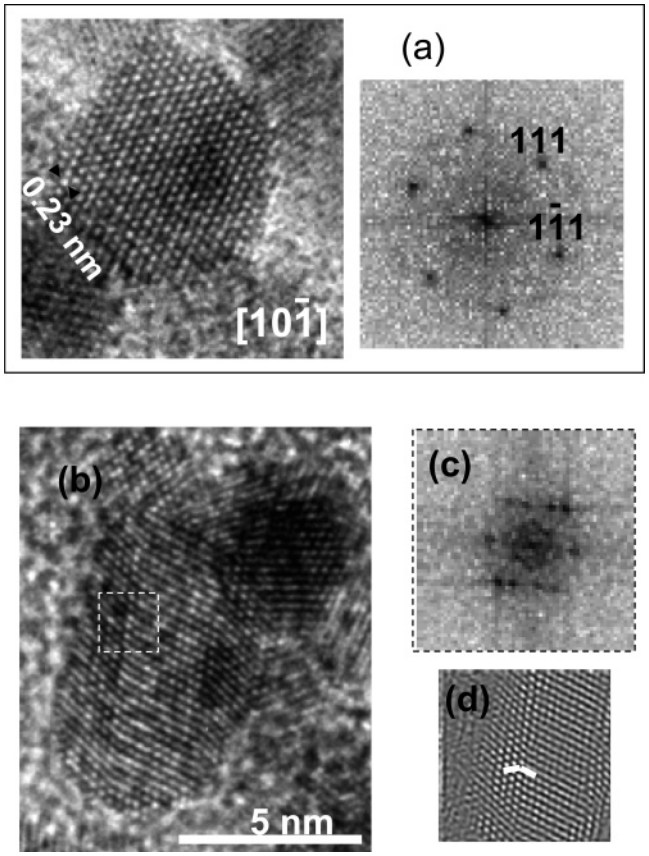

Figure 3. (a) HREM image and corresponding FFT of a Pt nanocrystal along the [10$\bar{1}$] zone axis. The fcc structure is evident. (b) HREM image of a twinned Pt nanocrystal along the [10$\bar{1}$] zone. (c) Corresponding FFT. (d) IFFT. The twin boundary is more clearly seen after noise subtraction.

periodicities (Figure 3a), along the [10$\bar{1}$] zone axis, are in agreement with the Pt fcc structure.[11] Additional structural features due to the existence of rotated domains, i.e., twinning (Figure 3b), are frequently found. A similar situation has been recently described for Pd nanoparticles.[6] For a better understanding of the mentioned defect, the fast Fourier transform (FFT) was attained (Figure 3c). The splitting of the FFT spots, as a consequence of twinning, is evident. The two tilted domains are clearly seen at the corresponding inverse FFT (Figure 3d), where the twin boundary is marked. As Pt exhibits large surface anisotropy, the appearance of twin boundaries should decrease the surface energy. Due to the small size of the NP, the surface energy is a significant fraction of the total energy of the particle. The twin boundary formation energy for fcc metals is rather small, and thus, the formation of twin boundaries may decrease the total energy, explaining the large amount of twin boundaries observed in the micrographs.

Both features observed by TEM, the narrow range particle size of 2−5 nm and the presence of twin boundaries in these Pt NPs, may be associated with two fundamental aspects of the laser ablation technique employed for their synthesis. First, the presence of an observed intense plasma plume, as expected from the high irradiance values mentioned earlier in the Experimental Section, ensures a selective, high-energy transformation process for the starting compound. This is in

(11) JCPDS pattern 00-004-0802.

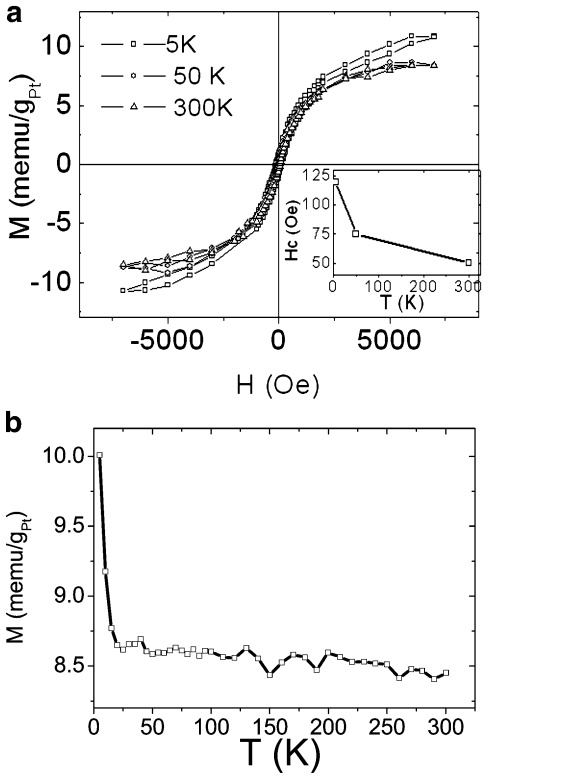

Figure 4. (a, top) Hysteresis loops of Pt nanoparticles at different temperatures. The inset shows the evolution of the coercive force with temperature. (b, bottom) Thermal dependence of magnetization under an applied field of 5 kOe.

contrast with the conventional high-temperature thermal decomposition processes, characteristic of methods which employ readily available heating technologies, and is likely responsible for the narrow particle size distribution observed. Second, the extremely fast cooling rates imposed by this method result in products which are in thermodynamically metastable states,[12] are amorphous in nature,[13] or, if highly crystalline, incorporate significant defects. Twinning is, in fact, consistently observed in crystalline materials prepared by similar laser techniques.[14] In addition, the fact that the laser is scanned over the sample on a preferential direction for the method reported here may provoke defects within the resulting product which appear anisotropically distributed along that direction.

Figure 4a shows the hysteresis loops at different temperatures ranging from 5 to 300 K. As can be observed, the NPs exhibit ferromagnetic-like behavior (i.e., hysteresis and coercivity) in the whole range of temperatures measured. The coercivity decreases as a function of the temperature from 120 Oe at 5 K to 50 Oe at 300 K, as shown in the inset. The thermal dependence of the magnetization was measured under an applied field of 5000 Oe (Figure 4b). A sharp decrease up to 20 K (about 15% of the value at 5 K) is observed, whereas it slightly diminishes as *T* increases from 20 to 300 K. The results pointed out that the blocking

(12) Larrea, A.; Snoeck, E.; Badía, A.; de la Fuente, G. F.; Navarro, R. *Physica C* **1994**, *220*, 21. Vasiliu, F.; Sarbu, C.; Parvulescu, V. I. *Solid State Ionics* **1997**, *95*, 107. Gervais, M.; Le Floch, S.; Gautier, N.; Massiot, D.; Coutures, J. P. *Mater. Sci. Eng.* **1997**, *B45*, 108.
(13) de la Fuente, G. F.; Beltrán, D.; Ibáñez, R.; Martínez, E.; Beltrán, A. *J. Less-Common Met.* **1989**, *150*, 253.
(14) Llorca, J.; Orera, V. M. *Prog. Mater. Sci.* **2006**, *51*, 711.

temperature for Pt NPs should be over 300 K, becoming the fingerprint of a huge anisotropy.

From these results, the magnetic moment for the Pt atom is 0.00042 μ_B if we assume all the atoms to participate equally in the magnetization. Such a small value suggests that only a few atoms contribute to the observed ferromagnetic behavior with a higher local magnetic moment.

When one deals with such low magnetic moments, potential impurity effects must always be taken into consideration. However, chemical analysis showed that the Fe content is below 0.01 atom %. Above and beyond the value of the magnetic moment, the presence of magnetic impurities could never explain the magnetic thermal behavior observed for these NPs. According to EDS measurements, no segregation of iron NPs was observed after analysis of more than 100 NPs. Therefore, the Fe impurities, if present, should be dispersed within the Pt nanoparticles. As the HREM study confirmed that the particle size was below 5 nm (which corresponds to ~5000 atoms), the number of Fe atoms per particle must be below 1. Even if some atoms were aggregated, forming 5 nm NPs, they would be superparamagnetic above 10 K. Moreover, if we assume Fe impurities to be 0.01 atom %, the magnetization associated with those impurities should be around 10^{-3} emu/g, 1 order of magnitude below the measured one. Actually, the latter value is consistent with the sharp decrease in magnetization observed in Figure 4b. Superparamagnetic impurities could thus be related to this low-temperature behavior, as even a single Fe atom can exhibit a blocking temperature due to the anisotropy enhancement induced by Pt atoms onto their surroundings,[15] but never to the ferromagnetic behavior observed at higher temperatures.

According to the experimental observations summarized in Figure 4a, the Pt nanoparticles exhibit permanent magnetic moments that give rise to the measured remanence. This feature is not observed in bulk Pt samples with similar Fe impurity levels. These behave as an enhanced Pauli paramagnet and are close to being ferromagnetic. Pt exhibits a high density of states at the Fermi level, $N(E_F) = 0.9$ eV^{-1},[16] but the Stoner parameter, I, ranges between 0.6 and 1, so the Stoner criterion ($N(E_F)I \geq 1$) is almost satisfied. The permanent magnetic moment may be induced by the local enhancement of the density of states at the neighborhood of the twin boundaries, observed by the HREM study (Figure 3). The rupture of cubic symmetry prevents the $t_{2g}-e_g$ splitting of the d bands, yielding a local d band narrowing that, as has been recently shown for Pd NPs, can be strong enough to hold the Stoner criterion.[6,17,18]

Charge transfer in Pt−carbon could also contribute to induce localized magnetic moments at the surface of the NPs as is the case for thiol-capped gold NPs.[7] Figure 5 shows the optical absorption spectra of Pt NPs where a band at 240 nm can be observed. This band is ascribed to the surface plasmon resonance, a collective oscillation of the conduction electrons inside the nanoparticle.[19] The width of this absorption band strongly depends on the particle volume where electrons can oscillate. The shape of the measured plasmon band corresponds to an oscillation volume equivalent to the particle size, according to TEM micrographs, confirming that most of the electrons in the NP are delocalized, exhibiting metallic behavior. However, the presence of localized states cannot be completely discarded.

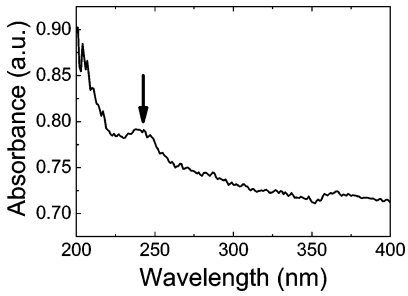

Figure 5. Optical absorption spectra of Pt nanoparticles. The surface plasmon resonance band is clearly observed at about 245 nm.

Regarding the origin of the huge anisotropy inferred from the thermal dependence of the magnetization, the blocking temperature over 300 K indicates that the anisotropy must be larger than 2.5×10^7 J m^{-3}, or 2.3 meV atom^{-1}.

While such a value is very high for crystalline anisotropy, the large spin−orbit coupling of Pt (about 1.5 eV) can account for this anisotropy and therefore for the hysteresis and coercivity observed up to temperatures above 300 K. The reduced symmetry at the twin boundaries can orient the angular magnetic moments in certain directions to distribute the local charge in the minimum energy configuration. The intense spin−orbit coupling could then orient the spin magnetic moments in this direction, as recently observed for the case of Co atoms deposited onto Pt surfaces.[15]

Conclusions

This work reports on the synthesis and magnetic properties of Pt nanoparticles (2−5 nm size NPs) derived from a commercial organometallic Pt compound. The use of a convenient laser ablation synthesis method allows NPs with physical properties which differ substantially from those of bulk Pt to be obtained. Both Pt NP characteristics, narrow particle size range and twinning, as confirmed by TEM observations, are attained as a consequence of the high-intensity plasma and drastic cooling rates associated with the laser synthesis method employed.

The first experimental observation of ferromagnetic behavior for carbon-coated platinum NPs, with coercivity up to room temperature, is also reported here. Measurements of the surface plasmon resonance show the presence of itinerant electrons within these NPs. TEM studies confirmed that Pt NPs exhibit a large concentration of twin boundaries, which reduce their surface energy. The lack of cubic

(15) Gambardella, P.; Rusponi, S.; Veronese, M.; Dhesi, S. S.; Grazioli, C.; Dallmeyer, A.; Cabria, I.; Zeller, R.; Dederichs, P. H.; Kern, K.; Carbone, C.; Brune, H. *Science* **2003**, *300*, 1130.
(16) Gunnarsson, O. *J. Phys. F: Met. Phys.* **1976**, *6*, 587.
(17) Paulus, P. M.; Goossens, A.; Thiel, R. C.; Van der Kraan, A. M.; Schmid, G.; de Jongh, L. J. *Phys. Rev. B* **2001**, *64*, 205418.
(18) Alexandre, S. A.; Anglada, E.; Soler, J. M.; Yndurain, F. Unpublished work. In this work the authors show from ab initio calculations that ferromagnetism in Pd nanoparticles can be explained as due to twin boundaries.
(19) Kreibig, U.; Völlmer, M. *Optical properties of metal clusters*; Springer-Verlag: Berlin, 1995.

symmetry at the twin boundaries could give rise to permanent magnetic moments. The large spin−orbit coupling of platinum accounts for a huge magnetic anisotropy and, thus, for the surprisingly high blocking temperature observed (>300 K). Possible Fe impurities cannot explain the large coercivity observed and reported at these temperatures.

Acknowledgment. This work has been partially supported by The Spanish Ministry for Education and Science through Projects NAN2004-09125-C07-05 and MAT2004-01248 and by the local Government of Aragón through its Consolidated Research Group Programme.

CM061740V